Biological Joint Loading and Exoskeleton Design

Roberto Leo Medrano, Elliott J. Rouse, Gray Cortright Thomas

***Abstract*—While assistive exoskeletons typically focus on the metric of metabolic cost, we hypothesize that exoskeletons of sufficient power density could also reduce knee joint loading, which is understood to be a risk factor for osteoarthritis. Using biomechanical locomotion data, we run a simple simulation of two types of exoskeletons: those that provide a parallel load-path to ground, and those that apply torque directly to the human knee joint. We find that the second type offers larger reductions at normal walking speeds and that the power density required for knee load reduction is much lower than for metabolic cost reduction.**

***Index Terms*—osteoarthritis, exoskeletons, wearable robots, knee joint, locomotion, internal forces**

I. Introduction

Assistive lower-body exoskeletons have been used to augment performance, but they could potentially protect against injury as well. These exoskeletons have the potential to reduce mechanical loading on the wearer's biological joints—a use case that could benefit those at risk of osteoarthritis (OA). Pain resulting from OA presents an obstacle to activities of daily living, and OA is a leading cause of chronic disability in older people [1]. Age and obesity act as major risk factors for the development of knee OA [2]. Additionally, athletes, first responders and members of the armed forces experience significantly higher rates of knee OA than equivalent control groups [3]. Although the exact etiology for knee OA is still unclear, it is generally agreed that increased or unusual mechanical loading due to obesity, occupational activities, or participation in impact sports plays an important role in the development and progression of knee OA [4].

Many exoskeletons today are designed to reduce the metabolic rate during locomotion [5]. This metric has been embraced by the field as its standard for success for how well the exoskeleton is assisting the wearer. Designs that are carefully engineered for high power density have achieved reductions on the order to 10% [6].

Some exoskeletons are potentially able to reduce knee loading by offering a parallel load path to ground, thereby offloading part of the mass of the load from the wearer [7]. A more nuanced benefit can also be conferred by applying torque assistance to the wearer's knee joint, as this can indirectly reduce muscle activation, and thus joint loading, due to reduced muscle force (shown as F_m in Fig. 1). Researchers have already noted that reduction of joint load is a potential benefit of providing assistive joint torque [8]–[10]. However, to our knowledge, a quantitative investigation into how exoskeleton design affects knee joint loading has yet to be explored.

In this paper we provide simulation-based evidence in support of the hypotheses that 1) exoskeletons can expect to achieve total joint load reduction at various locomotion speeds and 2) the power density required to reduce total joint load is less than that required to reduce the metabolic rate of the wearer. Our analysis includes two different exoskeleton architectures and quantifies their ability to attenuate knee forces during locomotion at different regimes of walking speed and exoskeleton power. Our model predicts that exoskeletons could reduce knee loading even with lower (*i.e.* worse) power densities than are demonstrated in modern systems designed to reduce the metabolic rate of the wearer. High power density increases design costs for exoskeletons, so a lower requirement could ultimately lead to higher rates of adoption.

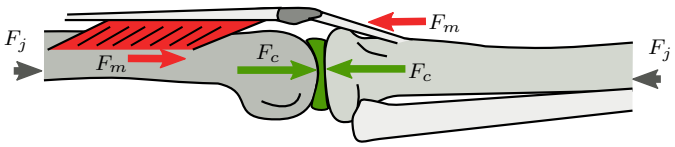

Fig. 1. **Components Involved in Joint Loading**—The total compression load on the joint, F_c, is the sum of the joint reaction force, F_j, and the muscular force, F_m, which is necessary to produce a torque about the human's joint. This second term, F_m, is typically larger than F_j, as indicated by the arrow scales.

II. Modeling

A. Biomechanical Model

We consider a simple mathematical model that describes how exoskeletons influence the magnitude of knee loads when they apply a scaled version of biological human torques. The model features a 75 kg (M_h) human undergoing payload carriage of a 34 kg load (M_p), at speeds ranging from 0.5 to 5 m/s.

The total contact force (F_c) on the knee is the sum of two forces: the *net joint reaction force*, F_j, resulting from the ground reaction force (GRF) and the *net muscular force*, F_m, resulting from the leg muscles generating a moment via musculotendon tension that loads the joint (Fig. 1). To obtain F_m from the knee torque, we assumed a constant moment arm about the knee of 0.03 meters [11]. We assume no co-activation of agonist-antagonist muscles spanning the knee joint, which would add additional loading not considered by our model. This assumption is supported by the limited co-activation observed in human subject experiments [12]. For loaded walking, we found that our simple model predicts peak joint loads within one standard deviation of the estimates in [11], [13], which use more complex models with individual muscle forces.

B. Model Data

To calculate the load on the knee joint at different speeds, we gathered published gait profile data to estimate the unloaded joint reaction force $F_{j,u}$ and unloaded muscular force

$F_{m,u}$ throughout the gait-cycle across different speeds [14]–[16]. The profiles for $F_{m,u}$ were determined by dividing the absolute value of net knee joint torques [14], [15] by our constant moment arm. The profiles for $F_{j,u}$ were calculated in one of two ways: for walking speeds, we used joint reaction force data directly from [15], while for running speeds, we used the GRF data from [16], which can be used to approximate the joint reaction forces [17]. We used this approach because direct data for $F_{j,u}$ was available for walking speeds but unavailable for running speeds, which necessitated this assumption and the use of readily available GRF data. Using these profiles, we interpolated a surface depicting the gait-cycle over a fine array of speeds between 0.5 and 5 m/s, featuring walking locomotion between 0.5 and 2 m/s, running locomotion between 2 and 5 m/s, and a discontinuity between the two forms at 2 m/s. Additionally, we obtained the average positive joint power for the knee joint ($P_{u,knee}$) and for the sum of the knee, hip, and ankle joints ($P_{u,total}$) across these different speeds, for later use in calculating exoskeleton mass [18].

To model the effects of increased borne mass from the exoskeleton and payload at a given speed, we scaled the corresponding $F_{j,u}$ and $F_{m,u}$ profiles for that speed by the ratio of that additional mass to the human mass. This yielded the muscle loading forces $F_{m,l}$ and reaction forces $F_{j,l}$ that represent loaded walking; these forces can be reduced through the action of the exoskeleton. Additionally, we assumed that the human's lower-limb kinematics depended only on speed and not on mass, as kinematics vary little with payload carriage [19]. This allowed us to model torque, and thus force, as directly proportional to power.

C. Exoskeleton Model

We identified two exoskeleton architectures that show the potential to mitigate knee forces during loaded walking: pure-torque exoskeletons, which apply assistance as pure torques about the joint of interest [6], [10], [20], [21], and parallel exoskeletons, which offload the forces of the payload to the ground through a parallel structure [22]–[26]. Our pure-torque exoskeleton model actuates solely the two knee joints in the sagittal plane, while our parallel model actuates six sagittal plane lower-body joints: hip, knee, and ankle for both legs. We discarded an alternative soft exosuit architecture that provides torque through artificial tendons, as these tendons also load the joint, resulting in a negligible benefit to joint loads relative to the pure-torque architecture.

We modelled the exoskeleton controller as providing a scaled version of the biological joint torques of an unladen human walking at the same speed, irrespective of the payload. We call this scale factor the *exoskeleton power fraction* α, as the same scaling that applies to unladen joint torque applies to the unladen human joint power P_u in determining the exoskeleton's power requirements. For the parallel architecture, P_u was equal to the sum of the average positive power needed by the ankle, knee, and hip joints to rotate in the sagittal plane ($P_{u,total}$); for the pure-torque single-joint knee exoskeletons, only the knee joint positive power was included ($P_{u,knee}$). We then modelled the exoskeleton mass (M_e) as proportional to αP_u using a constant η (kg/W) equal to the inverse of the power-density of the exoskeleton, which was obtained from the best-in-class literature [6], [26]. Lower inverse power densities are beneficial because they require less device mass to provide powered assistance to the wearer.

The mass model is thus given by the following equations:

$$M_e = \begin{cases} \eta\alpha P_{u,total} & \text{for parallel, and} \\ \eta\alpha P_{u,knee} & \text{for pure-torque single-joint} \end{cases} \tag{1}$$

$$\eta = \begin{cases} 0.22 & \text{for parallel, and} \\ 0.17 & \text{for pure-torque single-joint} \end{cases} \tag{2}$$

The torque provided by both architectures is subtracted from the total torque needed to perform the task thus reducing the torque needed from the human and lowering the musculotendon forces loading the knee joint $F_{m,l}$. The parallel architecture additionally reduces joint reaction force $F_{j,l}$ because it applies its assistance through the parallel structure. This exoskeleton model is given by the following equations:

$$F_{m,l} = \left(\frac{M_h + M_p + M_e}{M_h} - \alpha\right) F_{m,u}, \tag{3}$$

$$F_{j,l} = \begin{cases} \left(\frac{M_h+M_p+M_e}{M_h} - \alpha\right) F_{j,u} & \text{for parallel, and} \\ \left(\frac{M_h+M_p+M_e}{M_h}\right) F_{j,u} & \text{for pure-torque,} \end{cases} \tag{4}$$

$$F_c = F_{m,l} + F_{j,l}. \tag{5}$$

Over a grid of locomotion tasks parametrized by speed and α for each exoskeleton architecture, we obtained the peak knee load for each task by taking the maximum of the F_c profile for that task. We then normalized these loads by the loads experienced during the corresponding locomotion task without any exoskeleton assistance. Performing this procedure for both exoskeleton architectures yields two surfaces that represent the maximum normalized load on the knee for all locomotion regimes. To prevent unrealistically large exoskeleton masses, we filtered these surfaces to include only exoskeletons that were within a mass threshold. By combining these surfaces—selecting the architecture at each combination that produced the lowest knee load—we obtained an overall surface that shows the optimal load-reducing exoskeleton architecture at each regime of locomotion.

We also investigated the hypothesis that knee load reduction is more easily achieved, when compared to metabolic cost reduction. We compared the impact of exoskeleton assistance from a pure-torque single-joint knee exoskeleton over a grid of combinations of inverse power densities (η) and exoskeleton power fractions (α). For each peak joint load in this grid, we subtracted the peak joint load experienced during the reference condition of unassisted walking at 1 m/s with a 34-kg payload, and divided by this unassisted load to express the assisted peak load as a normalized change in loading. To enable direct comparison with the metabolic cost metric, we used the Augmentation Factor [27] to predict the change in metabolic cost due to assistance from a single-joint ankle exoskeleton, a common architecture choice for cost reduction, over the same grid of inverse power densities and exoskeleton

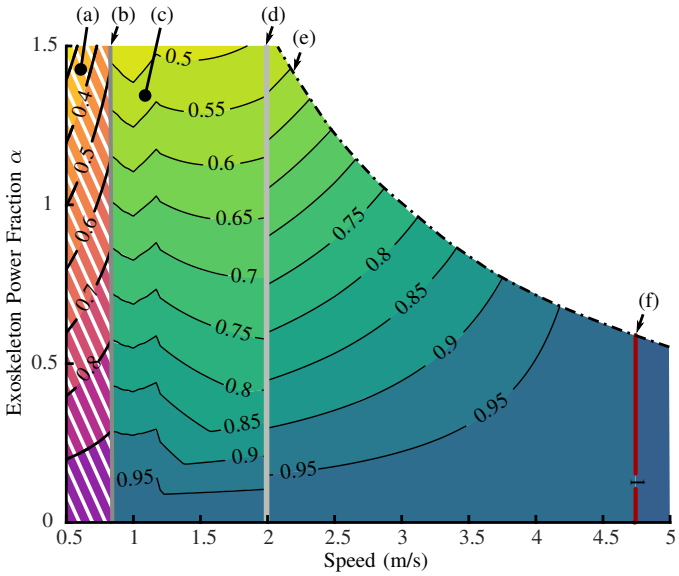

Fig. 2. **Fraction of knee joint load remaining due to simulated exoskeleton use in locomotion with a 34-kg backpack.** Regions (a) and (c) denote optimal use of parallel and pure-torque architectures respectively and are divided along the boundary (b). Boundary (d) separates walking from running gaits, boundary (e) marks a threshold on exoskeleton mass (1/3 the total system weight) that filters out unrealistically heavy exoskeletons, and boundary (f) marks the highest speed at which a pure-torque exoskeleton is capable of reducing knee loads. Both (e) and (f) are sensitive to power density, and (b) is related to the relative power densities of the two architectures.

powers. We again normalized the change in metabolism using unassisted walking at 1 m/s with a 34-kg payload [28].

III. Results

The two exoskeleton architectures—pure-torque and parallel–are expected to reduce knee loads below the unassisted case, denoted by the presence of normalized loads less than unity (Fig. 2). The combined surface, with isolines for clarity, represents the exoskeleton architecture that results in the lowest knee loads at each locomotion regime. The single-joint pure-torque exoskeleton dominates this combined surface (2-c) and is therefore the optimal choice for knee load reduction for most regimes. However, there exists a small but notable region at low speeds (2-a) in which parallel exoskeletons are the optimal choice.

The pure-torque region is bounded in α by the mass limitation (2-e). On the other hand, the intersection of the parallel and pure-torque regions (2-b) is determined by the relative advantages and disadvantages of each architecture, and how these facets change with speed. At around 4.7 m/s, the normalized load surface begins exceeding 1 (2-f), which denotes the point at which the pure-torque exoskeleton architecture can no longer aid the user in terms of knee load reduction, which is also fundamentally limited by the power-density of the architecture.

The hypothesis that joint load reduction is more readily achieved, when compared to metabolic cost reduction was supported (Fig. 3). Isolines with negative value represent a beneficial reduction from reference, whereas positive isolines denote a detrimental increase. At high exoskeleton power fractions, an inverse power density comparable to the state-of-the-art (≈0.17 kg/W) [6], and previously examined locomotion speeds (≈1 m/s), pure-torque single-joint exoskeletons are expected to reduce knee loads by 30%. The pure-torque architecture may even capable of reducing knee loads for high inverse power densities, whereas at a critical η value (≈0.24), the modelled pure-torque ankle exoskeleton is no longer capable of providing any metabolic benefit.

IV. Discussion

Pure-torque single-joint exoskeletons are capable of reducing joint loads over the largest range of speeds and power fractions due to their comparatively lower inverse power-density resulting in less device mass per unit power. The parallel exoskeletons, despite theoretically providing greater reduction of knee loads via weight offloading, suffer from a dramatic increase in mass at high speeds due to their higher inverse power-density, coupled with the higher power required to actuate all lower limb joints. More device mass is needed to deliver the same power during locomotion, which increases the total joint load at the knee and quickly penalizes parallel exoskeletons at higher speeds.

Single-joint pure-torque knee exoskeletons can still reduce knee joint loading even with inverse power densities that prohibit reduction of metabolic cost (>≈0.24 kg/W). The isolines for joint load reduction in Fig. 3a are relatively flat, demonstrating that the capacity for these devices to reduce joint loads is insensitive to power density. Strict power density requirements necessitate expensive materials and time-intensive design processes, and are therefore disadvantageous. Our model predicts that lower power densities can still render benefit to the user in terms of knee loading. And on this basis we hypothesize that *less expensive* exoskeletons with lower power densities can still provide a tangible benefit to wearers in the form of reducing knee loading, which may help prevent long-term debilitating diseases such as knee OA.

However, a practical question remains: will an exoskeleton designed to prevent OA by reducing joint loading inadvertently increase co-contraction and thereby reduce its efficacy? Our analysis neglected co-contraction; however, co-contraction has the potential to directly increase joint loading as agonist-antagonist muscle pairs simultaneously load the joint. If, in the implementation of an exoskeleton for joint load reduction, the human were to stiffen their joints—due to human uncertainty or discomfort—the total loading on the joint would increase and potentially outweigh the benefits of the device. Conversely, if the device causes biomechanical adaptations that reduce co-contraction, the exoskeleton could have a larger influence than we predict, especially with greater co-contraction observed during running [29].

Our analysis implicitly assumed that the exoskeleton provided torque in a profile similar to the biological torque needed during locomotion. Much effort has been spent optimizing exoskeleton torque profiles that reduce the metabolic rate of their wearers. Analogously, future work can determine optimal profiles that reduce knee loading, which may resemble pulses that actuate only when the total force at the knee exceeds

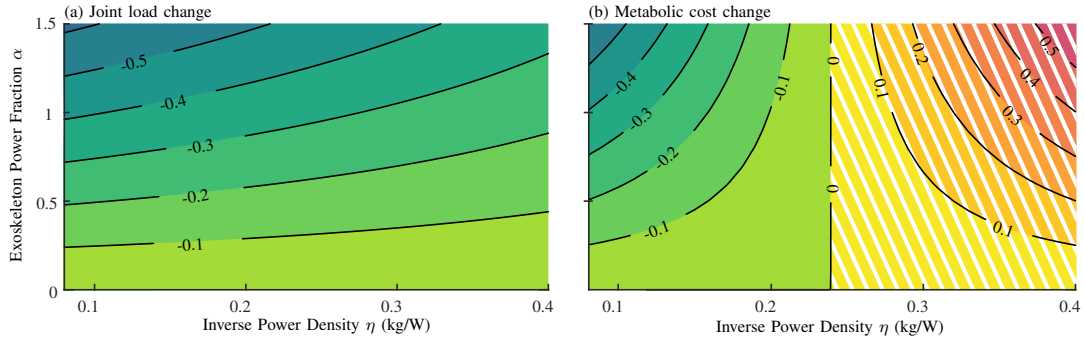

Fig. 3. **Effect of power density on change in joint loads and metabolic cost for pure-torque single-joint exoskeleton architecture, normalized by the reference condition of walking with a 34-kg payload at 1 m/s**—a) Change in knee joint loads from reference, normalized by the knee loads of the reference b) Change in metabolic cost from reference, normalized by the metabolic cost of the reference.

some threshold. This could further reduce the average power consumed by the exoskeleton, and thus its mass, while still protecting its wearer from knee loads.

References

[1] L. Sharma, S. Cahue, J. Song, K. Hayes, Y. C. Pai, and D. Dunlop, "Physical Functioning over Three Years in Knee Osteoarthritis: Role of Psychosocial, Local Mechanical, and Neuromuscular Factors," *Arthritis and Rheumatism*, vol. 48, no. 12, pp. 3359–3370, 2003.

[2] T. M. Griffin and F. Guilak, "The role of mechanical loading in the onset and progression of osteoarthritis," *Exercise and Sport Sciences Reviews*, vol. 33, no. 4, pp. 195–200, 2005.

[3] K. L. Cameron, J. B. Driban, and S. J. Svoboda, "Osteoarthritis and the tactical athlete: A systematic review," *Journal of Athletic Training*, vol. 51, no. 11, pp. 952–961, 2016.

[4] J. M. Vigdorchik, J. J. Nepple, N. Eftekhary, M. Leunig, and J. C. Clohisy, "What Is the Association of Elite Sporting Activities with the Development of Hip Osteoarthritis?," *American Journal of Sports Medicine*, vol. 45, no. 4, pp. 961–964, 2017.

[5] J. Kim, G. Lee, R. Heimgartner, D. A. Revi, N. Karavas, D. Nathanson, I. Galiana, A. Eckert-Erdheim, P. Murphy, D. Perry, N. Menard, D. K. Choe, P. Malcolm, and C. J. Walsh, "Reducing the metabolic rate of walking and running with a versatile, portable exosuit," *Science*, vol. 365, no. 6454, pp. 668–672, 2019.

[6] L. M. Mooney, E. J. Rouse, and H. M. Herr, "Autonomous exoskeleton reduces metabolic cost of human walking during load carriage," *Journal of NeuroEngineering and Rehabilitation*, vol. 11, no. 1, pp. 1–5, 2014.

[7] C. A. McGibbon, S. C. Brandon, M. Brookshaw, and A. Sexton, "Effects of an over-ground exoskeleton on external knee moments during stance phase of gait in healthy adults," *Knee*, vol. 24, no. 5, pp. 977–993, 2017.

[8] T. Lenzi, M. C. Carrozza, and S. K. Agrawal, "Powered hip exoskeletons can reduce the user's hip and ankle muscle activations during walking," *IEEE Trans. Neural Systems Rehabilitation Engineering*, vol. 21, no. 6, pp. 938–948, 2013.

[9] C. L. Lewis and D. P. Ferris, "Invariant hip moment pattern while walking with a robotic hip exoskeleton," *Journal of Biomechanics*, vol. 44, no. 5, pp. 789–793, 2011.

[10] H. Zhu, C. Nesler, N. Divekar, M. Ahmad, and R. Gregg, "Design and Validation of a Partial-Assist Knee Orthosis with Compact, Backdrivable Actuation," *IEEE Int. Conf. Rehab. Robot.*, 2019.

[11] S. P. Messier, C. Legault, R. F. Loeser, S. J. Van Arsdale, C. Davis, W. H. Ettinger, and P. DeVita, "Does high weight loss in older adults with knee osteoarthritis affect bone-on-bone joint loads and muscle forces during walking?," *Osteoarthritis and Cartilage*, vol. 19, no. 3, pp. 272–280, 2011.

[12] A. Khandha, K. Manal, J. Capin, E. Wellsandt, A. Marmon, L. Snyder-Mackler, and T. S. Buchanan, "High muscle co-contraction does not result in high joint forces during gait in anterior cruciate ligament deficient knees," *Journal of Orthopaedic Research*, vol. 37, no. 1, pp. 104–112, 2019.

[13] C. R. Winby, D. G. Lloyd, T. F. Besier, and T. B. Kirk, "Muscle and external load contribution to knee joint contact loads during normal gait," *Journal of Biomechanics*, vol. 42, no. 14, pp. 2294–2300, 2009.

[14] A. G. Schache, P. D. Blanch, T. W. Dorn, N. A. Brown, D. Rosemond, and M. G. Pandy, "Effect of running speed on lower limb joint kinetics," *Medicine and Science in Sports and Exercise*, vol. 43, no. 7, pp. 1260–1271, 2011.

[15] K. R. Embry, D. J. Villarreal, R. L. Macaluso, and R. D. Gregg, "Modeling the Kinematics of Human Locomotion over Continuously Varying Speeds and Inclines," *IEEE Trans. Neural Systems Rehabilitation Engineering*, vol. 26, no. 12, pp. 2342–2350, 2018.

[16] R. K. Fukuchi, C. A. Fukuchi, and M. Duarte, "A public dataset of running biomechanics and the effects of running speed on lower extremity kinematics and kinetics," *PeerJ*, vol. 2017, no. 5, p. 3298, 2017.

[17] E. S. Matijevich, L. M. Branscombe, L. R. Scott, and K. E. Zelik, "Ground reaction force metrics are not strongly correlated with tibial bone load when running across speeds and slopes: Implications for science, sport and wearable tech," *PLoS ONE*, vol. 14, no. 1, pp. 1–19, 2019.

[18] D. J. Farris and G. S. Sawicki, "The mechanics and energetics of human walking and running," *Journal of the Royal Society Interface*, vol. 9, no. 66, pp. 110–118, 2012.

[19] T. W. P. Huang and A. D. Kuo, "Mechanics and energetics of load carriage during human walking," *Journal of Experimental Biology*, vol. 217, no. 4, pp. 605–613, 2014.

[20] N. Riaz, S. L. Wolden, D. Y. Gelblum, and J. Eric, "Experimental Implementation of Underactuated Potential Energy Shaping on a Powered Ankle-Foot Orthosis," vol. 118, no. 24, pp. 6072–6078, 2016.

[21] G. Lv, H. Zhu, and R. Gregg, "On the design and control of highly backdrivable lower-limb exoskeletons," *IEEE Control Systems Mag.*, vol. 38, no. 6, pp. 88–113, 2018.

[22] C. J. Walsh, D. Paluska, K. Pasch, W. Grand, A. Valiente, and H. Herr, "Development of a lightweight, underactuated exoskeleton for load-carrying augmentation," *Proc. 2006 IEEE Int. Conf. Robotics and Automation*, no. May, pp. 3485–3491.

[23] A. Zoss, H. Kazerooni, and A. Chu, "On the mechanical design of the Berkeley Lower Extremity Exoskeleton (BLEEX)," *Proc. 2005 IEEE/RSJ Int. Con. Intelligent Robots and Systems*, pp. 3132–3139.

[24] M. Fontana, R. Vertechy, S. Marcheschi, F. Salsedo, and M. Bergamasco, "The body extender: A full-body exoskeleton for the transport and handling of heavy loads," *IEEE Robotics and Automation Magazine*, vol. 21, no. 4, pp. 34–44, 2014.

[25] T. Ishida, T. Kiyama, K. Osuka, G. Shirogauchi, R. Oya, and H. Fujimoto, "Movement analysis of power-assistive machinery with high strength-amplification," *Proc. SICE Annual Conf.*, pp. 2022–2025, 2010.

[26] H. Kazerooni, "Exoskeletons for human power augmentation," *2005 IEEE/RSJ Int. Conf. Intelligent Robots and Systems*, pp. 3120–3125.

[27] L. M. Mooney, E. J. Rouse, and H. M. Herr, "Autonomous exoskeleton reduces metabolic cost of walking," *Proc. 2014 Int. Conf. IEEE Engineering in Medicine and Biology Society*, vol. 11, no. 1, pp. 3065–3068.

[28] G. J. Bastien, P. A. Willems, B. Schepens, and N. C. Heglund, "Effect of load and speed on the energetic cost of human walking," *European Journal of Applied Physiology*, vol. 94, no. 1-2, pp. 76–83, 2005.

[29] T. F. Besier, M. Fredericson, G. E. Gold, G. S. Beaupré, and S. L. Delp, "Knee muscle forces during walking and running in patellofemoral pain patients and pain-free controls," *Journal of Biomechanics*, vol. 42, no. 7, pp. 898–905, 2009.